JOURNAL OF AIRCRAFT
Vol. 47, No. 4, July–August 2010

Engineering Notes

Vibration Analysis of Elastic Uniform Cantilever Rotor Blades in Unsteady Aerodynamics Modeling

Mir Y. Ziabari* and Behzad Ghadiri†
Tarbiat Modares University, 14117-1775 Tehran, Iran

DOI: 10.2514/1.45851

Nomenclature

A	=	blade cross-sectional area equations, m^2
a	=	lift-curve slope, 2π/rad
b	=	number of blades
C	=	blade chord, m
$[c]$	=	modal damping matrix
$C(k)$	=	Theodorsen's function
C_{d0}	=	drag coefficient
D	=	profile drag per unit length, N/m
E	=	Young's modulus, N/m^2
G	=	Shear modulus, N/m^2
h	=	vertical displacement normal to freestream velocity component V, m
I_2, I_1	=	cross-sectional area moments of inertia about the y' and z' axes, respectively, m^4
J	=	torsional stiffness constant, m^4
K_A	=	polar radius of gyration, m
K_m	=	mass radius of gyration, m
$[k]$	=	modal stiffness matrix
L	=	lift per unit length, N/m
L_u, L_v, L_w	=	aerodynamic forces per unit length
M	=	moment per unit length, N · m/m
$[M]$	=	modal mass matrix
M_ϕ	=	moment per unit length, N · m/m
m	=	mass per unit length, kg/m
R	=	blade length, m
$\bar{R}$	=	flap-lag structural coupling parameter
T	=	aerodynamic force per unit length, normal to blade airfoil chord line, N/m
U	=	airfoil velocity with respect to fluid, m/s
u, v, w	=	elastic axis displacements in (x, y, z), m
V_i	=	induced flow velocity
X, Y, Z	=	unreformed coordination system, m
$\bar{x}$	=	dimensionless length, x/R
α	=	airfoil section angle of attack, radian
α_j	=	constants for assumed mode shapes
β_j	=	constants for assumed mode shapes
β_{pc}	=	Pricon angle, rad
γ_j	=	constants for assumed mode shapes
θ	=	blade pitch angle, rad
θ_{cr}	=	blade pitch angle in stable condition, rad
κ	=	dimensionless tensional rigidity
Λ_1, Λ_2	=	dimensionless bending stiffness
ξ, η, ζ	=	deformed coordination system, m
φ	=	elastic torsion deflection about x axis, rad
ψ	=	dimensionless time, Ωt
Ω	=	rotor-blade angular velocity
$()'$	=	$\partial/\partial x$
$(\cdot)$	=	$\partial/\partial t$

Received 5 June 2009; revision received 26 February 2010; accepted for publication 27 March 2010.

*Master of Science, Department of Mechanical Engineering, Aerospace Division, Aerospace Engineering Department, Chamran Highway; y.ziabari@namvaran.com.

†Assistant Professor, Department of Mechanical Engineering, Aerospace Division, Aerospace Engineering Department, Chamran Highway; ghadiri@modares.ac.ir.

I. Introduction

AN ORDINARY problem related to the vibration analysis of helicopters that contain blade–body coupling is a single blade rotating and its effects on the whole building blocks in the study of helicopter dynamics. This study indicates that unfavorable instability usually occurs due to the coupled flap bending and torsion deflections, with a frequency near the torsion natural frequency. Furthermore, another type of instability occurs in the case of the hingeless rotor blade because of the structural coupling between bending and torsion deflections of cantilever blades. Considering unsteady aerodynamic equations and the basic general equations of motion related to the cantilever blade will cause nonlinearities, such as external flow in inertial and structural terms in the final equations of motion. These nonlinearities may be expected to cause a nonlinear blade motion behavior. The perturbation equations will be obtained by linearizing the nonlinear equations about a suitable equilibrium condition for finding a suitable first step of iteration. The influence of the nonlinear terms appears in the coefficients of the linear perturbation equations.

The complete nonlinear equations are solved via the numerical methods. In this paper, a second-order linear stability analysis based on linearization of the general improved nonlinear equations of motion has been investigated for unsteady aerodynamics.

II. Literature Review

Hodges and Ormiston [1] have developed a system of nonlinear flap-lag-torsion equations of motion for an elastic torsionally flexible cantilever blade and applied them to a cantilever blade stability analysis. However, the developed equations contain some errors because the effects of incorrect shear strain displacement were neglected. Hodges and Dowell [2] have applied the developed equations to a nonuniform rotor blade of a solid cross section, without a Pricon blade. In this case, most hingeless rotor configurations with uniform blade properties were found to be stable for typical bending and torsion frequencies. Hodges and Ormiston [1] have provided the results for a broad range of system parameters and illustrated the general stability characteristics of hingeless rotors by changing basic assumptions [3]. A theoretical analysis has been primarily developed by Hodges [4] for analyzing the aeromechanical stability of bearingless rotor helicopters, concerning hover motion (air resonance) and ground resonances. Stephens et al. [5] have presented a mixed formulation for calculating a static equilibrium and stability eigenvalues of nonuniform rotor blades in hover motions. Kwon et al. [6] have analytically determined a coupled flap-lag-torsion aeroelastic stability and response of hingeless rotors in the hovering flight condition. They have represented the surface of the rotor blades by a number of quadrilateral panels, with the uniform source and doublets.

Shang et al. [7] have developed the geometrically exact nonlinear beam and the generalized dynamic wake theories based on a finite-element technique, forming a precise and compact formulation. An

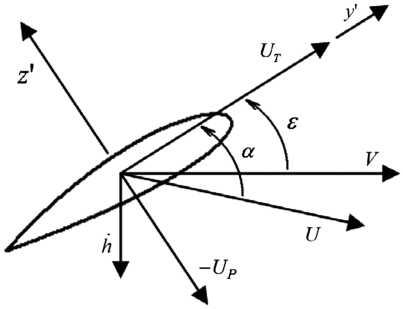

Fig. 1 Rotor-blade airfoil section.

analytical model for predicting the aeroelastic behavior of composite rotor blades, concerning straight and swept tips, has been presented by Friedmann et al. [8]. They have not considered the effect of coupling between the flap, torsion, and bending displacements. The rotating blade has been modeled by finite elements along the elastic axis, using the Hamilton's principle. They have shown that the composite ply orientation has a substantial effect on blade stability. Compatibility between a composite beam cross-sectional analysis and a helicopter rotor-blade model has been studied by Friedmann et al, using a finite-element cross-sectional analysis code [9]. Finally, the investigation on stability of the curved beam has been studied by Chang and Hodges [10].

III. Structural and Inertial Terms

Concerning the Hamilton principal, the basic equations of motion are obtained by [3]. These equations are modified for the blades, having uniform mass and stiffness without twist and chordwise offsets of the elastic axis. Modifications for the equations are made to accommodate an approximate structural coupling parameter.

Governing equations for flap-bending motion are mathematically described as

$$
\begin{aligned}
&-\frac{1}{2}m\Omega^2[(R^2-x^2)v']' - 2m\Omega\left(v'\int_x^R \dot{v}\,\mathrm{d}x\right)' \\
&\quad + (EI_1\sin^2\theta + EI_2\cos^2\theta)v'''' + (EI_2 - EI_1)(\sin\theta\cos\theta)w'''' \\
&\quad + (EI_2 - EI_1)[-(v''\phi)''\sin 2\theta + (w''\phi)''\cos 2\theta] \\
&\quad + m(\ddot{v} - \Omega^2 m) - 2m\Omega\int_0^R (v''\dot{v}' + w'\dot{w}')\,\mathrm{d}x \\
&\quad - 2m\Omega\beta_{\mathrm{pc}}\dot{w} = L_v
\end{aligned}
\tag{1}
$$

The equation of motion for the lead-lag motion is as follows:

$$
\begin{aligned}
&-\frac{1}{2}m\Omega^2[(R^2-x^2)w']' - 2m\Omega\left(w'\int_x^R \dot{v}\,\mathrm{d}x\right)' \\
&\quad + (EI_1 cis^2\theta + EI_2\sin^2\theta)w'''' + (EI_2 - EI_1)(\sin\theta\cos\theta)v'''' \\
&\quad + (EI_2 - EI_1)[(v''\phi)''\cos 2\theta + (w''\phi)''\sin 2\theta] \\
&\quad + m\ddot{w} + 2m\Omega\beta_{\mathrm{pc}}\dot{v} = L_w - 2m\Omega^2\beta_{\mathrm{pc}}x
\end{aligned}
\tag{2}
$$

The equation of motion for torsion is:

$$
\begin{aligned}
&-GJ\phi'' - \tfrac{1}{2}m\Omega^2 k_A^2[(R^2-x^2)\phi']' \\
&\quad + (EI_2 - EI_1)[\sin\theta\cos\theta(w''^2 - v''^2) + \cos 2\theta v''w''] \\
&\quad + m\Omega^2(k_{m2}^2 - k_{m1}^2)\phi\cos 2\theta + mk_m^2\ddot{\phi} \\
&\quad = M_\phi - \Omega^2 m(k_{m2}^2 - k_{m1}^2)\sin\theta\cos\theta
\end{aligned}
\tag{3}
$$

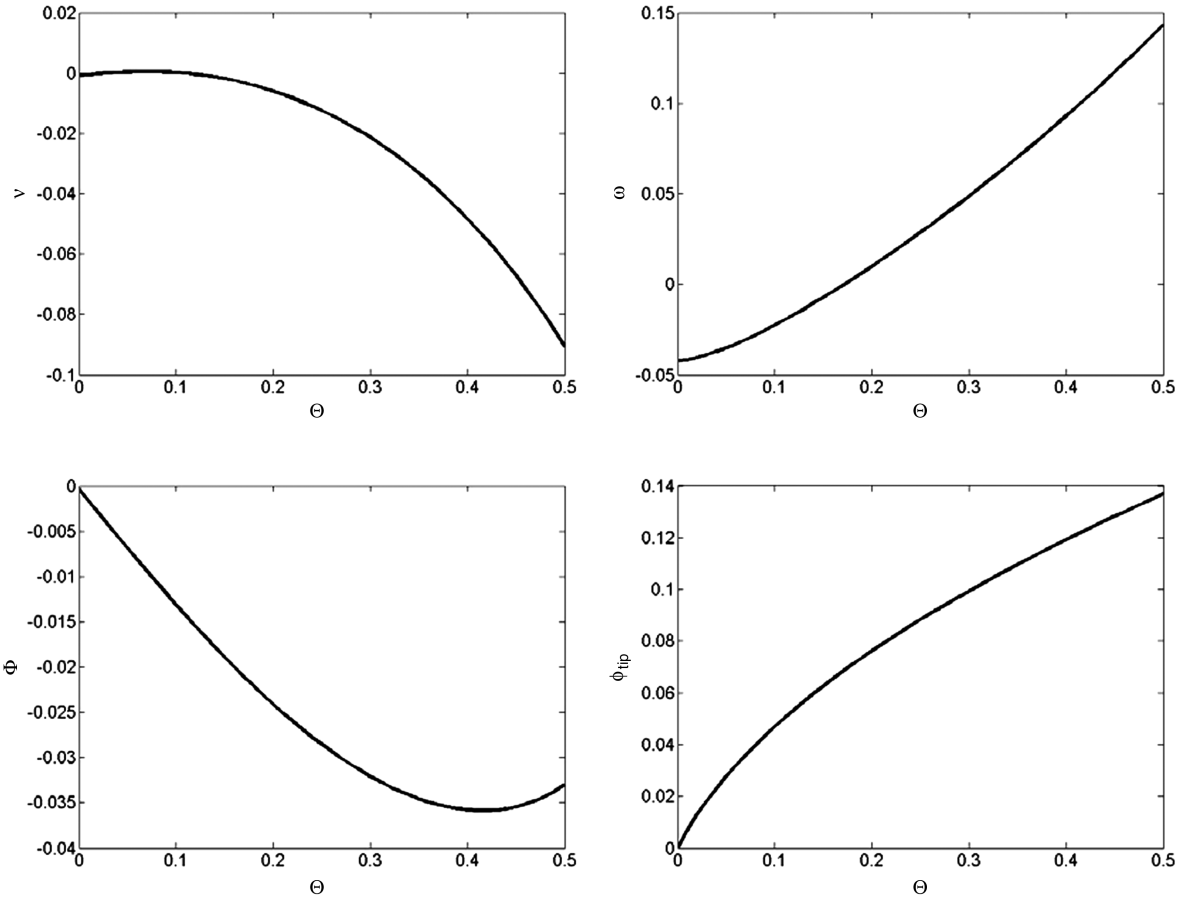

Fig. 2 Deflected blade in $\Lambda_1 = 0.0105$, $\Lambda_2 = 0.1$, $\kappa = 0.0018$, and $\beta_{\mathrm{pc}} = 0.05$.

Table 1 Values of α_j and β_j [14]

Parameters	Values	Parameters	Values	Parameters	Values	Parameters	Values
α_1	0.7341	α_4	1.00003	β_1	1.8751	β_4	10.9955
α_2	1.01847	α_5	1	β_2	4.69401	β_5	14.1372
α_3	0.99922	α_6	1	β_3	7.85486	β_6	17.2788

Table 2 Values of configurations [3]

$N = 6$	$\Lambda_2 = 0.024, 0.1, 0.166$
$\frac{Cd_0}{Cl_\alpha} = 0.001592$	$\Lambda_1 = 0.00105$
$n = 4$	$\kappa = 0.0011, 0.0058$
$\bar{C} = \frac{c}{R} = 0.07854$	$(\frac{k_A}{k_m})^2 = 1.5$
$\sigma = 0.1$	$\theta = 0 \rightarrow 0.5$
$\frac{k_{m1}}{k_{m2}} = \frac{\mu_1}{\mu_2} = 0$	$\beta_{pc} = 0, 0.05, 0.1$
$\frac{k_m}{R} = \mu = 0.025$	$\gamma = 5$
	$\bar{R} = 1$

The above equations are nonlinear integro-partial-differential equations with variable coefficients in x.

IV. External Aerodynamic Forces

Based on Greenberg's method [11] for a low frequency, the aerodynamic force and moment coefficients on the blade will be calculated using the strip theory. Greenberg has extended the Theodorsen's theory for pulsating freestream velocity $V(t)$. The lift force and pitching moment may be expressed in terms of the circulatory and noncirculatory components:

$$L = L_C + L_{NC}; \qquad M = M_C + M_{NC} \tag{4}$$

Concerning Fig. 1, the noncirculatory lift force and moment about the airfoil pivot axis (analogous to the rotor-blade elastic axis) are given by

$$L_{NC} = \frac{c\rho_\infty ac}{8}\left(\ddot{h} + V\dot{\varepsilon} + \dot{V}\varepsilon + \frac{c}{4}\ddot{\varepsilon}\right)$$

$$\text{and} \qquad L_c = \frac{V\rho_\infty ac}{2}\left(\dot{h} + V\varepsilon + \dot{V}\varepsilon + \frac{c}{2}\dot{\varepsilon}\right);$$

$$M_{NC} = -\frac{cL_{NC}}{4} - \frac{\rho_\infty ac}{2}\left(\frac{c}{4}\right)^3\frac{\ddot{\varepsilon}}{2}$$

$$\text{and} \qquad M_C = -\frac{\rho_\infty ac}{2}\left(\frac{\dot{c}}{4}\right)^2 V\dot{\varepsilon} \tag{5}$$

Final equations are presented on the basis of two-dimensional unsteady aerodynamic modeling. A detailed explanation for the development of equations is presented in [12]:

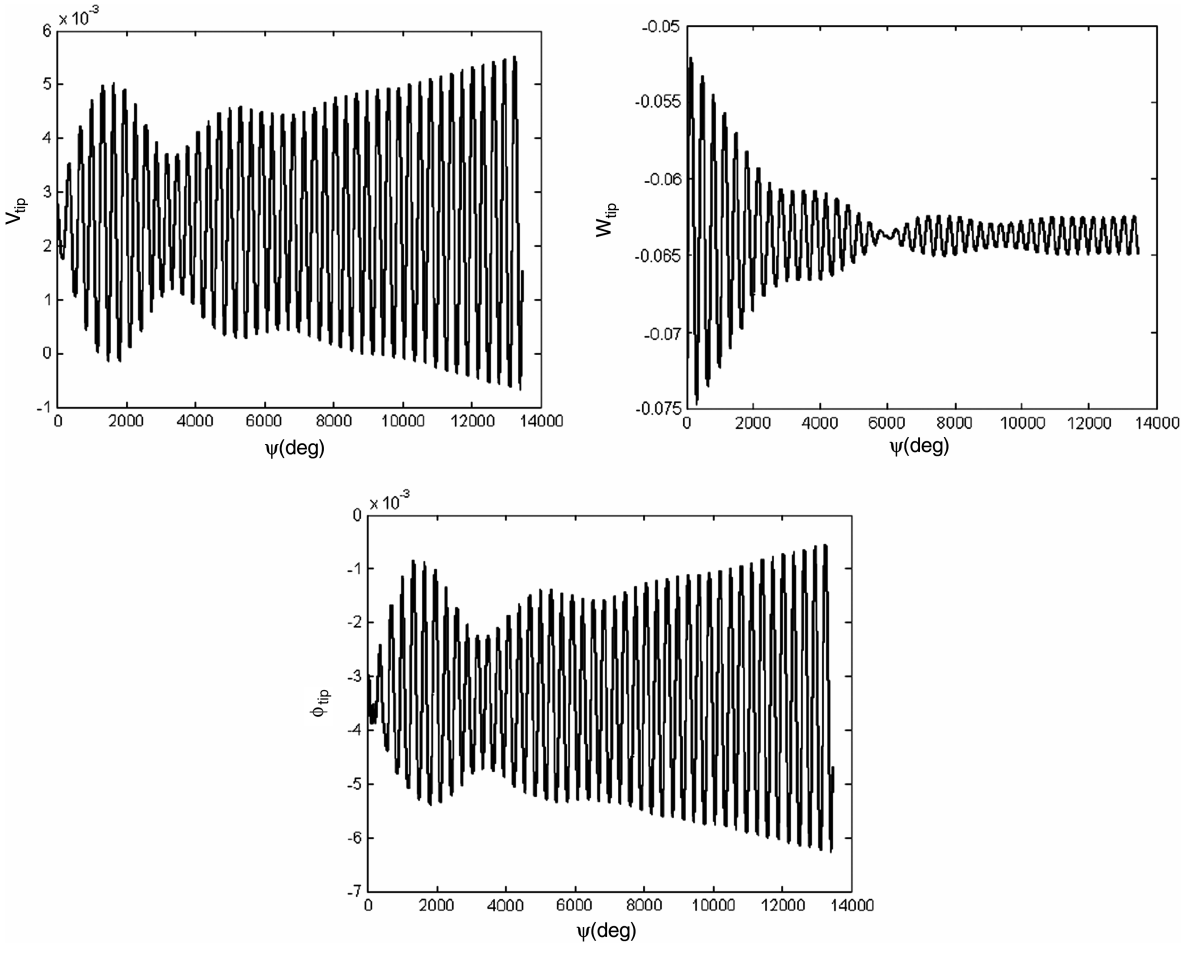

Fig. 3 Vibration blade for $\Lambda_1 = 0.0105$, $\Lambda_2 = 0.1$, $\kappa = 0.0018$, $\beta_{pc} = 0.05$, and $\theta = 0.21$.

$$L_v = cl_\alpha \rho b \left\{ V_i^2 V_i \Omega x(\theta+\phi) - \Omega x(\theta+\phi)\dot{w} - V_i(\theta+\phi)\dot{v} + 2V_i\dot{w} - \frac{c_{d0}}{cl_\alpha} U_\infty \Omega x - \frac{c_{d0}}{cl_\alpha} U_\infty \dot{v} \right\} \tag{6}$$

$$L_w = cl_\alpha \rho b \left\{ -\Omega x V_i + \Omega^2 x^2 \left(\theta + \phi + \int_0^x v' w' \, \mathrm{d}x \right) - \Omega^2 x v(\beta_{\mathrm{pc}} + w') + \Omega^2 x b(\beta_{\mathrm{pc}} + w') + [2\Omega x(\theta+\phi) - V_i]\dot{v} - \Omega x \dot{w} + \frac{3b}{2}\Omega x \dot{\phi} - \frac{b}{2}\ddot{w} \right\} \tag{7}$$

$$M_\phi = -\pi \rho b^2 \Omega x \phi \tag{8}$$

$$\bar{V}_i = \mathrm{sign}\left[\theta + \phi_{(\mathrm{st})}(0.75\bar{R})\Omega\bar{R}\frac{\pi\sigma}{8} \times \left(\sqrt{1 + \frac{12}{\pi\sigma}\{\theta + \phi_{(\mathrm{st})}(0.75\bar{R})\}} - 1 \right) \right] \tag{9}$$

V. Solution of the Equations of Motion

Final flap-lag-torsion equations of motion will be obtained by combining Eqs. (1–3) and (6–8). The Galerkin's method, with six coupled rotating mode shapes near the equilibrium operating condition, will be used for solving these integro-partial-differential equations.

Galerkin's method will lead to reducing the equations of motion to ordinary differential equations. In this regard, the form of dimensionless bending and torsion deflections ($\bar{V} = V/R$, $\bar{W} = W/R$) shall be changed into the terms of a series with generalized coordinates and mode shape functions:

$$\bar{v} = \sum_{j=1}^{N} V_j(\psi)\Psi_j(\bar{x}) \qquad \text{and} \qquad \bar{w} = \sum_{j=1}^{N} W_j(\psi)\Psi(\bar{x})$$

$$\text{and} \qquad \phi = \sum \phi_j(\psi)\Theta_j(\bar{x}) \tag{10}$$

This operation yields to 3N modal equations in terms of generalized coordinates V_j, W_j, and ϕ_j. The assumed mode shapes for the bending and torsion deflections are the standard nonrotating and uncoupled mode shapes for a uniform cantilever beam [3] with complementaries, as in Table 1:

$$\Psi_j(\bar{x}) = \cosh(\beta_j\bar{x}) - \cos(\beta_j\bar{x}) - \alpha_j[\sinh(\beta_j\bar{x}) - \sin(\beta_j\bar{x})]; \qquad \Theta_j(\bar{x}) = \sqrt{2}\mathrm{Sin}(\gamma_j\bar{x}); \qquad \gamma_j = \pi(j - 1/2) \tag{11}$$

By arranging the equations as an ordinary vibration equation (X), deflection will be estimated in each iteration step with the solving of Eq. (12) and each step result will be employed for the next iteration. Therefore, M, C, K, and F matrices are functions of blade location. Then, the updated previously mentioned matrices will be implemented for the next step, with the help of Table 2. Here, $[M]$ is symmetric, but $[C]$ and $[K]$ are asymmetric and depend on V_j, W_j, and ϕ_j:

$$M\ddot{X} + C\dot{X} + KX = F \tag{12}$$

$$X = \begin{Bmatrix} V_j \\ W_j \\ \phi_j \end{Bmatrix}; \qquad j\text{: 1–6} \tag{13}$$

VI. Results

Solving the equations of motions needs a suitable guess as the first step of iteration. Furthermore, in this paper, the vibration analysis has

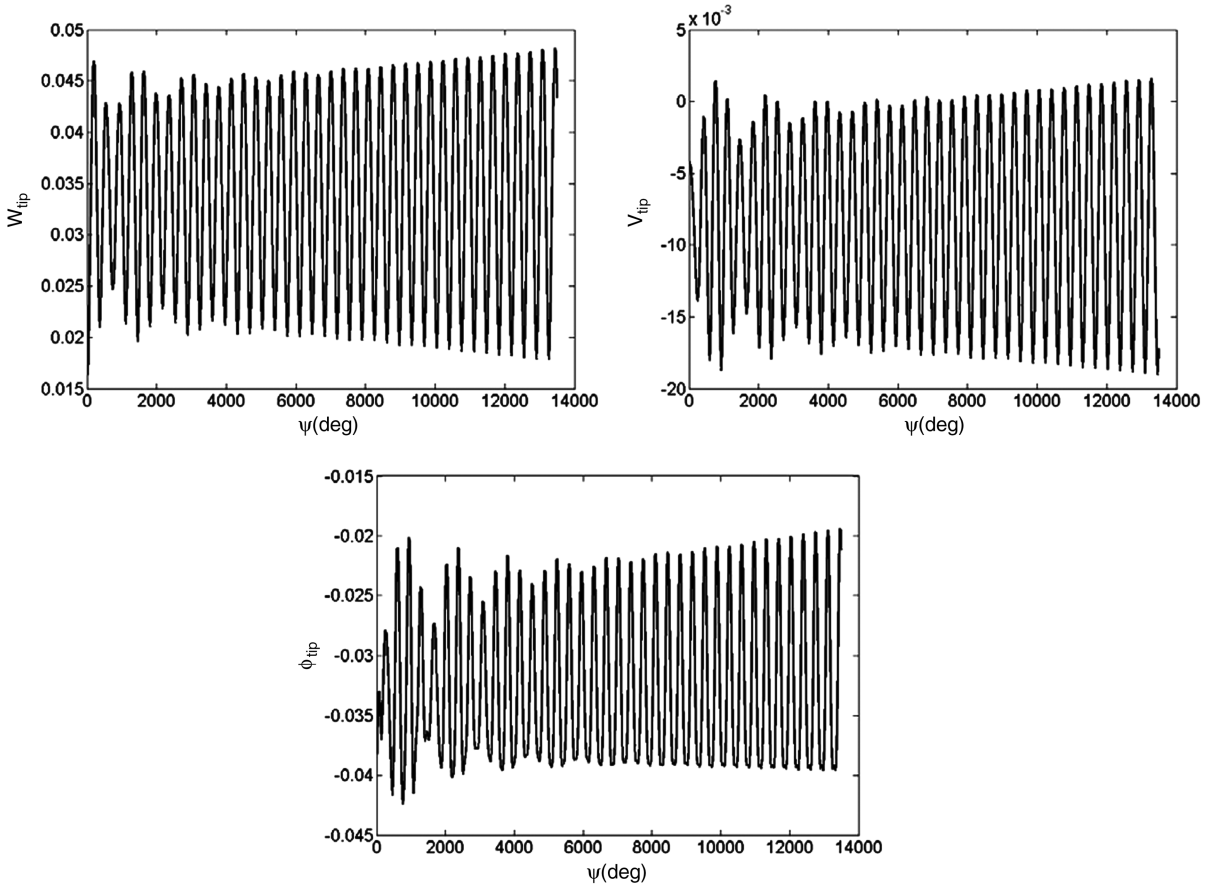

Fig. 4 Vibration blade in $\Lambda_1 = 0.0105$, $\Lambda_2 = 0.1$, $\kappa = 0.001$, $\beta_{\mathrm{pc}} = 0.0$, and $\theta = 0.2$.

been considered near the equilibrium operating condition, so the equations of motion are required to solve in steady-state conditions. Equation (14) presents a useful expression for determining the steady-state deflections, which are functions of pitch angle based on [4]. The results are given in terms of dimensionless tip deflections:

$$\bar{v}_{(\mathrm{st})\mathrm{tip}} = 2\sum_{j=1}^{N} V_{(\mathrm{st})j}(-1)^{j+1}$$

$$\text{and} \qquad \bar{w}_{(\mathrm{st})\mathrm{tip}} = 2\sum_{j=1}^{N} W_{(\mathrm{st})j}(-1)^{j+1}$$

$$\text{and} \qquad \phi_{(\mathrm{st})\mathrm{tip}} = \sqrt{2}\sum_{j=1}^{N} \phi_{(\mathrm{st})j}(-1)^{j+1} \tag{14}$$

The presented method in [12], the results for the steady-state deflection, and the induced flow velocity V_i will be graphically illustrated in Fig. 2.

Solving the equations of motion will result in a general overview of the stability curves for hingeless rotor-blade flap-lag torsion with the constant blade pitch angle θ. The procedure to obtain the results is presented in [12]. The repetitive solution of motion equations will indicate on uncoupled modes related to flap and lead lag at a zero pitch angle. Consequently, the flap mode is highly damped because of external forces, such as aerodynamic force and moments. Meanwhile, the lead-lag damping is very small, but it is always stable because of small aerodynamic drag forces associated with lead-lag velocity. By increasing the blade pitch angle, the coupling between flap and lead lag, which will cause instability, will increase, as in Fig. 3.

Torsional flexibility will cause the changes in flap-lag stability characteristics. Referring to [12], these changes can be large in the case of low-torsion frequency. The soft in-plane lead-lag mode damping is generally increased by torsional flexibility, while the flap mode damping is reduced. As torsional flexibility increases, the increase in lead-lag damping would be due to the equivalent kinematic pitch-lag coupling produced by bending-torsion structural coupling, as in Fig. 4.

Dimensionless equations of motion for rotating blades are employed to find final solutions independent of rotating speed and blade specifications. Meanwhile, they shall be considered in dimensionless parameter quantities.

Repetitive extracting results indicate a rotating blade instability appearance on $\theta = 0.195$ rad.

VII. Results Verification

The instability boundary condition is obtained from the following process for several pitching angles. The flutter pitch angle in constant rotating speed is calculated by solving the extracted equations repeatedly.

Considering blade specifications, as presented in Eq. (15), the flutter phenomenon will take place at $\theta = 0.195$ rad. Comparing with the results, which are graphically illustrated in Fig. 9 of [13], indicates a 1.4% discrepancy:

$$\Lambda_1 = 0.0105; \qquad \Lambda_2 = 0.1; \qquad \kappa = 0.001; \qquad B_{\mathrm{pc}} = 0 \tag{15}$$

Parts of this discrepancy are because of uncertainties existing in structural and aerodynamic assumptions; uncertainties that will be caused by using Galerkin's and Greenberg's methods for developing aerodynamic forces.

VIII. Conclusions

Extracted results and conclusions are listed as follows:

1) For low values of rotating speed, the stability will occur by increasing a torsion frequency. However, for higher torsion, frequency will make the system stable.

2) The order of accuracy is a function of the number of mode shapes, which are chosen for solving the equations of motion. For solving equations in coupled rotating mode shapes, selection of six mode shapes seems to be enough, but for less mode shapes, it may obtain incorrect results.

3) Increasing the Pricon angle is more effective than raising the collective pitching angle in instability appearances. Involving a small amount of the Pricon angle may cause large displacements in a rotating blade.

4) For low-pitch angles, the flap mode is highly damped because of external forces, such as aerodynamic forces. Meanwhile, the lead-lag damping is very small, but it is always stable because of small aerodynamic drag forces associated with a lead-lag velocity.

5) By increasing the blade pitch angle, the coupling between the flap and lead-lag increases; this event may cause instability.

6) The increasing of drag forces will cause the stability of the rotating blade because of the increase in the drag forces in the damping matrices.

References

[1] Hodges, D. H., and Ormiston, R. A., "Stability of Elastic Bending and Torsion of Uniform Cantilevered Rotor Blades in Hover," 14th Structures, Structural Dynamics, and Materials Conference, AIAA Paper 1973-405, March 1973.

[2] Hodges, D. H., and Dowell, E. H., "Nonlinear Equations of Motion for the Elastic Bending and Torsion of Twisted Nonuniform Rotor Blades," NASA TN D-7818, 1974.

[3] Hodges, D. H., and Ormiston, R. A., "Stability of Elastic Bending and Torsion of Uniform Cantilever Rotor Blades with Variable Structural Coupling," NASA TN D-8192, 1976.

[4] Hodges, D. H., "A Theoretical Technique for Analyzing Aeroelastic Stability of Bearingless Rotors," *AIAA Journal*, Vol. 17, No. 4, April 1979, pp. 400–407. doi:10.2514/3.61139

[5] Stephens, W. B., Hodges, D. H., Avila, J. H., and Kung, R. M., "Stability of Nonuniform Rotor Blades in Hover Using a Mixed Formulation," NASA TM 81226, 1980.

[6] Kwon, O. J., Hodges, D. H., and Sankar, L. N., "Stability of Hingeless Rotors in Hover Using Three-Dimensional Unsteady Aerodynamics," *Journal of the American Helicopter Society*, Vol. 36, No. 2, April 1991, pp. 21–31. doi:10.4050/JAHS.36.21

[7] Shang, X., Hodges, D. H., and Peters, D. A., "Aeroelastic Stability of Composite Hingeless Rotors in Hover with Finite-State Unsteady Aerodynamics," *Journal of the American Helicopter Society*, Vol. 44, No. 3, July 1999, pp. 206–221. doi:10.4050/JAHS.44.206

[8] Friedmann, P. P., Yuan, P. K. A., and Terlizzi, M. d., "An Aeroelastic Model for Composite Rotor Blades with Straight and Swept Tips," *International Journal of Non-Linear Mechanics*, Vol. 37, Nos. 4–5, June 2002, pp. 967–986. doi:10.1016/S0020-7462(01)00109-3

[9] Friedmann, P. P., Glaz, B., and Palacios, R., "A Moderate Deflection Composite Helicopter Rotor Blade Model with an Improved Cross-Sectional Analysis," *International Journal of Solids and Structures*, Vol. 46, No. 10, 2009, pp. 2186–2200. doi:10.1016/j.ijsolstr.2008.09.017

[10] Chang, C., and Hodges, D. H., "Stability Studies for Curved Beams," *Journal of Mechanics of Materials and Structures*, Vol. 4, Nos. 7–8, 2009, pp. 1257–1270. doi:10.2140/jomms.2009.4.1257

[11] Greenberg, J. M., "Airfoil in Sinusoidal Motion in a Pulsating Stream," NACA TN 1326, 1947.

[12] Ziabari, M. Y., "Calculation of Dynamic Instability Speed Boundary in Rotating Blades of Helicopters," M.S.C. Dissertation, Mechanical Engineering Department Aerospace Div. Tarbiat Modares Univ., Tehran, Iran, 2008.

[13] Shahverdi, H., Nobari, A. S., Behbahani-Nejad, M., and Haddadpour, H., "Aeroelastic Analysis of Helicopter Rotor Blade in Hover Using an Efficient Reduced-Order Aerodynamic Model," *Journal of Fluids and Structures*, Vol. 25, No. 8, Nov. 2009, pp. 1243–1257. doi:10.1016/j.jfluidstructs.2009.06.007

[14] Felgar, R. P., Jr., *Formulas for Integrals Containing Characteristic Functions of a Vibrating Beam*, Univ. of Texas at Austin Austin, TX, 1950, Chap. 2.